


# On the Ground State of Pd<sub>13</sub>

Andreas M. Köster,<sup>†</sup> Patrizia Calaminici,<sup>†</sup> Emilio Orgaz,<sup>‡</sup> Debesh R. Roy,<sup>§</sup> José Ulises Reveles,<sup>§</sup> and Shiv N. Khanna<sup>\*,§</sup>

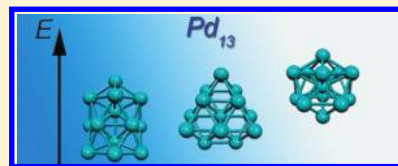
<sup>†</sup>Departamento de Química, Cinvestav, Avenida Instituto Politécnico Nacional 2508 A.P. 14-740, México D.F. 07000, México

<sup>‡</sup>Departamento de Física y Química Teórica, Facultad de Química, Universidad Nacional Autónoma de México, CP 04510, México D.F., México

<sup>§</sup>Department of Physics, Virginia Commonwealth University, Richmond, Virginia 23284-2000, United States

 Supporting Information

**ABSTRACT:** First-principles electronic structure calculations within a gradient corrected density functional formalism have been carried out to investigate the electronic structure and magnetic properties of Pd<sub>13</sub> clusters. It is shown that a bilayer ground-state structure that can be regarded as a relaxed bulk fragment is most compatible with the experimental results from Stern-Gerlach measurements. An icosahedral structure, considered to be the ground state in numerous previous studies, is shown to be around 0.14 eV above the ground state. A detailed analysis of the molecular orbitals reveals the near degeneracy of the bilayer or icosahedral structures is rooted in the stabilization by p- or d-like cluster orbitals. The importance of low-lying spin states in controlling the electronic and magnetic properties of the cluster is highlighted.



## 1. INTRODUCTION

Small atomic clusters are now known to constitute a new phase of matter where the properties can change radically with size, composition, and the charged state.<sup>1,2</sup> The geometrical structure, electronic character, magnetic coupling, and the chemical features can all be different from the bulk, and an important objective in cluster science is the determination of the atomic arrangement and the associated electronic configuration of the ground state and neighboring isomers. The clusters are generally too small for microscopy and too large for conventional spectroscopic techniques. Structure determination therefore has mostly proceeded through indirect approaches invoking synergism between theory and experiment.<sup>3</sup> For neutral magnetic clusters, one such approach is to combine Stern–Gerlach experiments with theory.<sup>4</sup> In these experiments, a beam of neutral magnetic clusters is passed through a gradient magnetic field that deflects the cluster. Because the magnetic anisotropy energies at small sizes are small, the clusters undergo superparamagnetic relaxations,<sup>5</sup> and the deflection is determined by the magnetization of the cluster in the field as well as the strength of the gradient field. Knowing the temperature and the field, one can deduce the magnetic moment (spin and orbital) that can be compared to theoretical calculations to ascertain the ground state. This approach is particularly powerful in cases where the ground state has close lying multiplet states. Because the cluster experiments are carried out at finite temperature, excitations to close lying spin states can alter the magnetic moment, and hence a measure of the magnetization can be used to further substantiate the determination of the theoretical findings.<sup>6</sup> In this Article, we demonstrate how this synergistic effort enables us to uniquely identify the ground state of a Pd<sub>13</sub> cluster.

Bulk palladium is a nonmagnetic metal. However, introduction of magnetic impurities like Fe in bulk is known to induce large host polarization in the surrounding atoms.<sup>7–10</sup> At small sizes, palladium clusters are found to be intrinsically magnetic with moments per atom that can approach that of a Ni site in bulk Ni. These findings have stimulated interest in palladium clusters, and a large number of theoretical and experimental efforts have been devoted to their studies.<sup>11–20</sup> The case of Pd<sub>13</sub> has attracted particular attention.<sup>11,15–20</sup> The earlier theoretical studies indicated that it has a compact icosahedral ground state with a spin magnetic moment of 8  $\mu_B$ .<sup>11–17</sup> However, more recent studies have challenged this structure assignment.<sup>18–20</sup> They yield bilayer or less compact three-dimensional structures with spin magnetic moments of 4<sup>18</sup> or 6  $\mu_B$ .<sup>19,20</sup> In general, the energy differences between the compact icosahedral and the less compact Pd<sub>13</sub> structures are small. Moreover, they seem to be method dependent as contradictory structure assignments suggest. Therefore, a more quantitative comparison between experiment and theory is needed for a reliable structure assignment of the Pd<sub>13</sub> ground state. Unfortunately, no direct experiments on the structure of Pd<sub>13</sub> exist. However, the magnetic moments of Pd<sub>13–105</sub> clusters have been measured using Stern–Gerlach deflection. These studies indicate an upper limit to the magnetic moment of around 5.2  $\mu_B$  for Pd<sub>13</sub>,<sup>21</sup> much less than the earlier predicted value for the icosahedral structure. Because a Stern–Gerlach experiment probes the total magnetic moment that includes the spin and orbital contributions, the spin magnetic moment alone may be expected to be reduced from 5.2  $\mu_B$ . Consequently, any determination of

Received: May 11, 2011

Published: June 28, 2011

the ground state must be able to reconcile with this observed low spin magnetic moment.

In this work, we have carried out a detailed investigation of the geometrical arrangement, electronic structure, and spin magnetic moment of the  $\text{Pd}_{13}$  cluster to identify the structure seen in experiments. Our studies focus on two key issues. (1) Unlike clusters of early transition metal atoms, does a  $\text{Pd}_{13}$  cluster have a nonicosahedral ground state? (2) Can the ground-state structures account for the low spin magnetic moment observed in experiments? In particular, what are the energy differences between different spin multiplicities? Our detailed studies, carried out within a gradient corrected density functional scheme, answer some of these questions. We identify the ground and other low energy spatial and spin states and show how they can account for the observed value of the magnetic moment at finite temperatures. Through detailed electronic structure investigations, we identify the electronic features that stabilize a nonicosahedral ground state.

## 2. THEORETICAL AND COMPUTATIONAL METHODS

The theoretical investigations are carried out within a gradient corrected density functional theory (DFT) framework.<sup>22,23</sup> A molecular orbital approach using a linear combination of atomic orbitals is applied to probe the electronic structure. The wave functions for the cluster were expressed as a linear combination of Gaussian-type orbitals (GTO) situated at the atomic positions in the cluster. The actual calculations were performed using the implementation in the deMon2k code.<sup>24</sup> For exchange and correlation functional, we have used a generalized gradient approximation (GGA) as proposed by Perdew, Burke, and Ernzerhof (PBE).<sup>25</sup> The palladium atom is described using a 18 electron quasi-relativistic effective core potential (QECP) and the corresponding valence basis set as proposed by Andrae et al.<sup>26</sup> To avoid spin contaminations, the restricted open-shell Kohn–Sham auxiliary density functional theory methodology is employed.<sup>27</sup> The auxiliary density was expanded in primitive Hermite Gaussian functions by using the GEN-A2\* auxiliary function set.<sup>28</sup> We have validated this methodology on the palladium atom and dimer. As shown in the Supporting Information, the auxiliary density functional theory description of the geometric and electronic structure of  $\text{Pd}_2$  is of good quality and compares favorably with available experimental data and CCSD(T) results.

To determine the geometry and spin multiplicity of the ground state, the configuration space was sampled by starting from several initial configurations and spin multiplicities and optimizing the geometry employing the quasi-Newton Levenberg–Marquardt method.<sup>29</sup> All structures were fully optimized in delocalized redundant coordinates without imposing any symmetry constraints, to allow for full variational freedom. The obtained minima were characterized by frequency analysis. To probe the thermal stability of some of the optimized structures, Born–Oppenheimer molecular dynamics (BOMD) simulations at the same level of theory were performed, too.

## 3. RESULTS AND DISCUSSION

Our theoretical studies indicate the presence of various low-lying energy structures for  $\text{Pd}_{13}$ . As global minimum, we find a septet (spin magnetic moment of  $6.0 \mu_{\text{B}}$ )  $C_s$  bilayer arrangement as depicted in Figure 1. Only 99 meV higher in energy is a septet  $C_{3v}$  bilayer minimum located. Above these two structures, a manifold of energetically low-lying bilayer structures with lower multiplicities is located. The relative energies are given in Table 1. As this table shows, the energetically closest icosahedral structure is a nonet (spin magnetic moment of  $8.0 \mu_{\text{B}}$ ). It represents a slightly distorted icosahedral structure ( $\sim I_h$ ) with Pd–Pd bonds

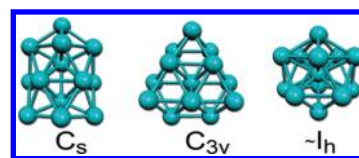


Figure 1. Topology of optimized  $\text{Pd}_{13}$  isomers.

Table 1. Relative Energies for the Relevant Multiplicities of the  $C_s$  and  $C_{3v}$  Bilayer Clusters and the Distorted Icosahedral ( $\sim I_h$ )  $\text{Pd}_{13}$  Clusters with Respect to the  ${}^7C_s$  Ground State in meV

structure	multiplicity				
	$m = 1$	$m = 3$	$m = 5$	$m = 7$	$m = 9$
$C_s$	158	128	104	0	213
$C_{3v}$	153	131	108	99	295
$\sim I_h$	774	630	523	341	134

ranging between 2.61 and 2.73 Å. Figure 1 shows all three minima topologies that are similar for all spin states given in Table 1. These results indicate a topological rich potential energy surfaces with multiple minima in various spin multiplicities for  $\text{Pd}_{13}$ . As mentioned before,  $\text{Pd}_{13}$  has been previously investigated by numerous authors using a variety of techniques.<sup>11–20</sup> Most authors have only considered the icosahedral structure and obtained a ground state with a spin magnetic moment of  $8.0 \mu_{\text{B}}$ ,<sup>11–17</sup> in agreement with current findings. Hafner and co-workers<sup>19</sup> did find a bilayer  $C_{3v}$  ground state as obtained in this work using the Vienna ab initio simulation package (VASP) code, while Wang et al.<sup>20</sup> report the  $C_s$  structure as the ground state using the same code. Both of the authors report a spin magnetic moment of  $6.0 \mu_{\text{B}}$ . Sun et al.<sup>16</sup> have also recently reported the elongated  $C_s$  structure as the ground state using a hybrid density functional.

While one could imagine multiple minima, none of these structures are compatible with the reported Stern–Gerlach results of  $\text{Pd}_{13}$ . The key pointer is that the observed magnetic moment is less than  $5.2 \mu_{\text{B}}$ . Because the clusters in the Stern–Gerlach are at finite temperatures, the key to the ground-state determination lies in the structure of the spin manifolds. To this end, we calculated the relative energy of the various spin states for the distorted icosahedral and the  $C_s$  and  $C_{3v}$  bilayer structures. These are given in Table 1. It is important to highlight that while the relative energies between two geometrical shapes could change with the choice of the functional and the numerical procedure, the relative ordering of the spin states for a given structure is less sensitive to these choices. Note that the lowest-energy state for the distorted icosahedral structure has a nonet multiplicity (spin magnetic moment of  $8.0 \mu_{\text{B}}$ ). The closest spin state is separated by 341 meV and has septet multiplicity. Higher multiplicities are separated by more than 1 eV and, therefore, are not relevant to our discussion here. On the other hand, the  $C_s$  and  $C_{3v}$  bilayer lowest-energy states with septet multiplicity have low-lying quintet, triplet, singlet, and, less close, nonet states. Higher multiplicities than the nonet are also for these both clusters not relevant. Because the clusters in Stern–Gerlach experiments are at finite temperatures, one can assume that these states are energetically accessible. To examine this quantitatively, we calculated the average magnetic moment for the different cluster structures using a simple Boltzmann distribution:

$$\langle \mu(T) \rangle = \sum_{m=1}^9 \frac{e^{-\Delta \varepsilon_m / RT}}{Q(T)} (m-1) \mu_B$$

The partition function is given by:

$$Q(T) = \sum_{m=1}^9 e^{-\Delta \varepsilon_m / RT}$$

Here,  $\Delta \varepsilon_m$  denotes the relative energies of the spin states with respect to the  ${}^7C_s$ ,  ${}^7C_{3v}$ , and  $\sim I_h$  lowest-energy states of the  $\text{Pd}_{13}$  cluster structures. The calculated  $\langle \mu(T) \rangle$  curves for the  $C_s$  (blue),  $C_{3v}$  (green), and  $\sim I_h$  (red)  $\text{Pd}_{13}$  structures are shown in Figure 2. For comparison, the experimental threshold value of  $5.2 \mu_B$  (dashed line) is also depicted in this figure. Note that a temperature

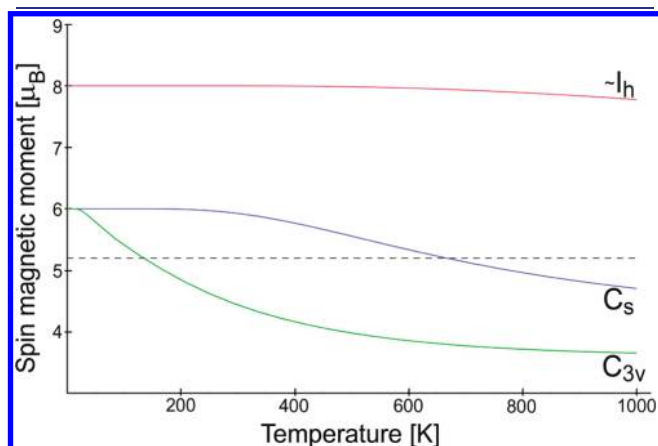


**Figure 2.** Spin magnetic moments of the  $C_s$  (blue),  $C_{3v}$  (green), and  $\sim I_h$  (red)  $\text{Pd}_{13}$  structures as a function of temperature. The horizontal line denotes the experimentally observed threshold for the cluster magnetic moment.

of 200 K would already reduce the calculated moment of the bilayer  $C_{3v}$  structure to values close to the experimental finding. The same holds for the  $C_s$  structure at around 700 K. On the other hand, the distorted icosahedral ( $\sim I_h$ ) structure shows only a very small temperature dependency of the magnetic moment and is far from the experimental threshold value over the entire temperature range. We would like to add that the Stern-Gerlach experiments are carried out on free clusters, and one has to consider the conservation of angular momentum. However, previous studies<sup>6</sup> have shown that the spin can couple to the rotations, and we believe that this combined with spin orbit coupling in Pd atoms provides the mechanism for the transition between the various spin states.<sup>30</sup>

At this point, it seems natural to ask the question about the interplay between the change of cluster multiplicity and structure. In Figure 3, density plots of the Boltzmann distributions at 100, 300, and 500 K for the three structures,  $C_s$ ,  $C_{3v}$ , and  $\sim I_h$  of  $\text{Pd}_{13}$ , considered here, are shown. The probability weight of a cluster structure is proportional to the shading of the corresponding field. As Figure 3 shows, both bilayer structures,  $C_s$  and  $C_{3v}$ , are significantly populated in the septet and quintet states even at

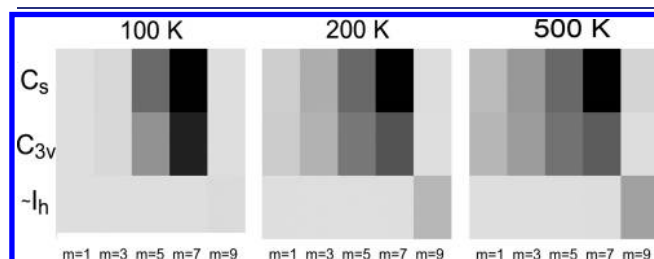


**Figure 3.** Boltzmann distributions for different temperatures of the  $\text{Pd}_{13}$  clusters listed in Table 1. The weight of a cluster structure is proportional to the shading of the corresponding field.

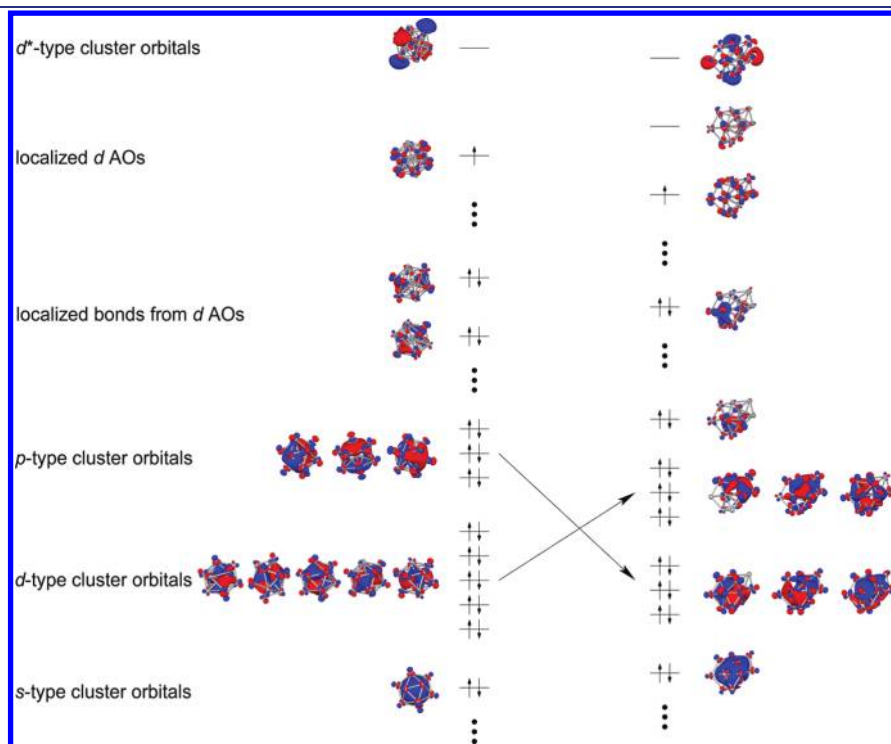


**Figure 4.** Molecular orbital correlation diagram between the  $\sim I_h$  (left) and  ${}^7C_s$  (right)  $\text{Pd}_{13}$  cluster. See text for details.



low temperature (100 K). With raising temperature, the lower multiplicities of these two structures are further populated. This is the reason for the above-discussed reduction of the spin magnetic moment with increasing temperature. However, Figure 3 also shows that at the same time both bilayer structures are populated. Hence, we propose that both bilayer structures in various spin states ranging from the singlet to the septet are observed in the Stern–Gerlach experiment. Thus, the reported experimental magnetic moment is an average of all of these states as depicted in Figure 3. This also naturally explains the observed noninteger value of  $5.2 \mu_B$  that lies between a quintet and septet state.

Figure 3 also indicates that at higher temperatures the  $\sim^9I_h$  Pd<sub>13</sub> structure gains population. Thus, the question arises if this structure might be also seen in experiment, obviously with a much lower population as the bilayer structures. To address this question, we performed canonical BOMD simulations at 500 K for the two lowest-energy bilayer states,  $^7C_s$  and  $^7C_{3v}$ . Starting from the minimum, we propagated each system for 20 ps. Along these trajectories, rearrangements to icosahedral topologies were not observed. We, therefore, conclude that icosahedral Pd<sub>13</sub> structures are not relevant to the reported Stern–Gerlach experiment.

An important question is the microscopic mechanism that stabilizes the bilayer structures as compared to the icosahedral shape. To this end, we examined the nature of molecular orbitals (MOs) of the  $\sim^9I_h$  and  $^7C_s$  Pd<sub>13</sub> clusters. Despite their different shapes, the qualitative orbital structure is similar and permits a molecular orbital correlation as shown in Figure 4. Both clusters possess a set of delocalized orbitals that extend over the full system. We name them cluster orbitals in analogy to their appearance in coin metal clusters.<sup>31,32</sup> Besides these cluster orbitals, localized d-type atomic orbitals (AOs) dominate the MO diagram of the clusters. As Figure 4 shows, the  $\sim^9I_h$  Pd<sub>13</sub> possesses s-, p-, and d-type cluster orbitals. However, their ordering is unusual as the d-type cluster orbitals are lower in energy than the p-type cluster orbitals. This situation changes in the  $^7C_s$  Pd<sub>13</sub> cluster as the arrows in Figure 4 indicate. In this cluster, only the low-lying s- and p-type cluster orbitals are well-defined. The d-type cluster orbitals mix with a manifold of localized bond orbitals and, therefore, are no longer well identifiable. Such localized bond orbitals also exist in smaller number in the icosahedral Pd<sub>13</sub> structure but are well separated from the cluster orbitals. This analysis indicates that the extra stabilization of the bilayer Pd<sub>13</sub> structures results from the stabilization of the p-type cluster orbitals, and the mixing of the d-type cluster orbitals with the localized bond orbitals. The importance of cluster orbitals for the Pd<sub>13</sub> structures is also demonstrated by the unoccupied d\*-type cluster orbital. Occupying this orbital substantially increases the cluster energy. This is the reason why multiplicities above the nonet, where this orbital must be occupied, are significantly higher in energy than the multiplicities discussed here. Our analysis shows that cluster orbitals, which determine the structure of the small coin metal clusters, are also of importance for late transition metal clusters.

## 4. CONCLUSIONS

To summarize, the present studies indicate that the ground state of an isolated neutral Pd<sub>13</sub> is a bilayer structure with a spin magnetic moment of  $6.0 \mu_B$ . The ground state is marked by several spin isomers within a few meV. Above the bilayer ground state is an icosahedral structure that is 134 meV less stable and has a spin magnetic moment of  $8 \mu_B$  with other spin multiplicities states that are higher in energy. The observed spin magnetic

moment of Pd<sub>13</sub> is therefore due to the clusters in the bilayer structure and excitation to close magnetic isomers at finite temperatures that leads to a low moment of  $5.2 \mu_B$  as observed in experiments. These results indicate that the total magnetic moment of a Pd<sub>13</sub> cluster not only undergoes superparamagnetic relaxations along various directions in space but also a change in the intrinsic magnetic moment is expected. A detailed analysis of the electronic states reveals that the bilayer structure is stabilized by cluster states with overall p-character while the icosahedral structure is marked by states with d-character. This raises the possibility that the relative stability of the two structures could be controlled by absorbing atoms that couple preferentially to p- or d-type cluster orbitals. In fact, our preliminary studies indicate that the addition of O atoms can reverse the stability of the two structures as O p-states hybridize preferentially with d-type cluster states. Such couplings provide an unprecedented ability to tune the atomic structure through external additions. We are in the process of exploring a variety of atoms that can stabilize one or the other structure and how such structural changes could correlate with catalytic behavior. These findings will form the basis of future publications.

## ■ ASSOCIATED CONTENT

**S Supporting Information.** The validation of the employed methodology on the palladium atom and dimer and the optimized Pd<sub>13</sub> cluster structures along with their total energies. This material is available free of charge via the Internet at <http://pubs.acs.org>.

## ■ AUTHOR INFORMATION

**Corresponding Author**  
snkhanna@vcu.edu

## ■ ACKNOWLEDGMENT

D.R.R., J.U.R., and S.N.K. gratefully acknowledge support by the Chemical Sciences, Geosciences and Biosciences Division, Office of Basic Energy Sciences, Office of Science, U.S. Department of Energy under Grant No. DE-FG02-11ER16213. P.C., E.O., and A.M.K. acknowledge funding from ICyTDF (PIFUTP08-87 and PICCO-10-47) and CONACyT (60117-U and 130726). Parts of the calculations were performed at the DGSCA-UNAM supercomputing facility and the WESTGRID, Canada.

## ■ REFERENCES

- (1) Kondow, T.; Kaya, K.; Terasaki, A., Eds. *Structures and Dynamics of Clusters*; Universal Academic Press, Inc.: Tokyo, 1996.
- (2) Khanna, S. N.; Castleman, A. W., Jr.; Eds. *Quantum Phenomena in Clusters and Nanostructures*; Springer: Germany, 2003.
- (3) Gutsev, G. L.; Khanna, S. N.; Jena, P. *Phys. Rev. B* **2000**, *62*, 1604–1606.
- (4) Khanna, S. N.; Rao, B. K.; Jena, P.; Knickelbein, M. *Chem. Phys. Lett.* **2003**, *378*, 374–379.
- (5) Khanna, S. N.; Linderroth, S. *Phys. Rev. Lett.* **1991**, *67*, 742–745.
- (6) Popov, A. P.; Pappas, D. P.; Anisimov, A. N.; Khanna, S. N. *Phys. Rev. Lett.* **1996**, *76*, 4332–4335.
- (7) Nieuwenhuys, G. J. *Adv. Phys.* **1975**, *24*, 515–595.
- (8) Cable, J. W.; David, L. *Phys. Rev. B* **1977**, *16*, 297–301.

- (9) Verbeek, B. H.; Nieuwenhuys, G. J.; Mydosh, J. A.; van Dijk, C.; Rainford, B. D. *Phys. Rev. B* **1980**, *22*, 5426–5440.
- (10) Reddy, V.; Khanna, S. N.; Dunlap, B. I. *Phys. Rev. Lett.* **1993**, *70*, 3323–3326.
- (11) Moseler, M.; Hakkinen, H.; Barnett, R. N.; Landman, U. *Phys. Rev. Lett.* **2001**, *12*, 2545–2548.
- (12) Kumar, V.; Kawazoe, Y. *Phys. Rev. B* **2002**, *66*, 144413.
- (13) Nava, P.; Sierka, M.; Ahlrichs, R. *Phys. Chem. Chem. Phys.* **2003**, *5*, 3372–3381.
- (14) Rogan, J.; García, G.; Valdivia, J. A.; Orellana, W.; Romero, A. H.; Ramírez, R.; Kiwi, M. *Phys. Rev. B* **2005**, *72*, 115421.
- (15) Aguilera-Granja, F.; Vega, A.; Rogan, J.; Orellana, W.; García, G. *Eur. Phys. J. D* **2007**, *44*, 125–131.
- (16) Sun, Y.; Fournier, R.; Zhang, M. *Phys. Rev. A* **2009**, *79*, 043202.
- (17) Barman, S.; Kanhere, D. G.; Das, G. P. *J. Phys.: Condens. Matter* **2010**, *21*, 396001.
- (18) Chang, C. M.; Chou, M. Y. *Phys. Rev. Lett.* **2004**, *93*, 133401.
- (19) Futschek, T.; Marsman, M.; Hafner, J. J. *Phys.: Condens. Matter* **2005**, *17*, S927–S963.
- (20) Wang, L.-L.; Johnson, D. D. *Phys. Rev. B* **2007**, *75*, 235405.
- (21) Cox, A. J.; Louderback, J. G.; Apsel, S. E.; Bloomfield, L. A. *Phys. Rev. B* **1994**, *49*, 12295–12298.
- (22) Hohenberg, P.; Kohn, W. *Phys. Rev. B* **1964**, *136*, B864.
- (23) Kohn, W.; Sham, L. J. *Phys. Rev. A* **1965**, *140*, A1133.1.
- (24) Köster, A. M.; Geudtner, G.; Calaminici, P.; Casida, M. E.; Dominguez, V. D.; Flores-Moreno, R.; Goursot, A.; Heine, T.; Ipatov, A.; Janetzko, F.; Martin del Campo, J.; Reveles, J. U.; Vela, A.; Zuniga, B.; Salahub, D. R. *The deMon Developers*; Cinvestav: México, 2011; see also <http://www.deMon-software.com>.
- (25) Perdew, J. P.; Burke, K.; Ernzerhof, M. *Phys. Rev. Lett.* **1996**, *77*, 3865–3868.
- (26) Andrae, D.; Haeussermann, U.; Dolg, M.; Stoll, H.; Preuss, H. *Theor. Chim. Acta* **1990**, *77*, 123–141.
- (27) Köster, A. M.; Reveles, J. U.; del Campo, J. M. *J. Chem. Phys.* **2004**, *121*, 3417–3424.
- (28) Calaminici, P.; Janetzko, F.; Köster, A. M.; Mejia-Olvera, R.; Zuniga-Gutierrez, B. *J. Chem. Phys.* **2007**, *126*, 044108.
- (29) Reveles, J. U.; Köster, A. M. *J. Comput. Chem.* **2004**, *25*, 1109–1116.
- (30) Schwarz, H. *Int. J. Mass Spectrom.* **2004**, *237*, 75–105.
- (31) Jug, K.; Zimmermann, B.; Calaminici, P.; Köster, A. M. *J. Chem. Phys.* **2002**, *116*, 4497–4507.
- (32) Jug, K.; Zimmermann, B.; Köster, A. M. *Int. J. Quantum Chem.* **2002**, *90*, 594–602.